

## Measuring the Single-Photon Temporal-Spectral Wave Function

Alex O. C. Davis,<sup>1</sup> Valérian Thiel,<sup>1</sup> Michał Karpiński,<sup>1,2</sup> and Brian J. Smith<sup>1,3</sup>

<sup>1</sup>*Clarendon Laboratory, University of Oxford, Parks Road, Oxford, OX1 3PU, United Kingdom*

<sup>2</sup>*Faculty of Physics, University of Warsaw, Pasteura 5, 02-093 Warszawa, Poland*

<sup>3</sup>*Department of Physics and Oregon Center for Optical, Molecular, and Quantum Science, University of Oregon, Eugene, Oregon 97403, USA*



(Received 21 February 2018; revised manuscript received 17 May 2018; published 21 August 2018)

Temporal-spectral modes of light provide a fundamental window into the nature of quantum systems and offer a robust means for information encoding. Methods to precisely characterize the temporal-spectral state of light at the single-photon level thus play a central role in understanding single-photon sources and their applications in emerging optical quantum technologies. Here we demonstrate an optical reference-free method, which melds techniques from ultrafast metrology and single-photon spectral detection, to characterize the pulse-mode structure of heralded single photons.

DOI: [10.1103/PhysRevLett.121.083602](https://doi.org/10.1103/PhysRevLett.121.083602)

The quantum state of a physical system, expressed as the wave function in the case of pure states, provides a complete description of the system and allows statistical predictions of measurement outcomes performed on it. The characterization of the quantum state plays a central role in the foundations of quantum physics and applications in quantum information science [1,2]. For a single photon, the quantum state is given by the electromagnetic field mode it occupies, which can be viewed as the photon wave function [3–5]. The various independent degrees of freedom of light can be used to encode information in the electromagnetic field, namely, transverse position-momentum [6], time frequency [7], and polarization [8]. Many demonstrations of quantum optical technologies have utilized polarization, path, or transverse-spatial mode encoding. These degrees of freedom are limited to relatively few quantum bits (qubits) that can be practically addressed within an integrated-optics platform, where high-stability, low-loss multiphoton interference, necessary for many optical quantum technologies, can occur. Recent research within quantum optics and quantum information science has focused on time-frequency encoding in ultrashort pulsed modes, stemming, in part, from the compatibility of pulsed modes with integrated optical platforms and the large information capacity of the time-frequency domain [9,10]. Ultrashort optical pulses are a key resource in modern physics and technology with applications ranging from precision metrology [11] and spectroscopy [12] to communications and control [13]. Their advantages are now being recognized for applications within optical quantum technologies, including quantum information processing [10,14], quantum-enhanced sensing [15], and quantum cryptography [16].

For a photon occupying given transverse-spatial and polarization modes, characterization of the temporal-spectral electromagnetic field mode completely determines

the single-photon state. There are several established techniques that enable the measurement of the mode of high-intensity pulses [17]. Among these are methods that utilize optical nonlinear interactions in the test field such as frequency-resolved optical gating [18] and spectral phase interferometry for direct electric field reconstruction [19]. However, at the single-photon level, these techniques are challenging to realize due to the weakness of optical nonlinear effects. Methods to measure the single-photon time-frequency state based on interference with known reference pulses in either a linear optical framework [20–22] or a nonlinear optical regime [23] have been recently demonstrated. These approaches require stable, tunable, well-characterized reference pulses for reliable measurements. Furthermore, techniques that utilize nonlinear interaction between a reference field and the single-photon state under examination require group-velocity- and phase-matching conditions to be satisfied, impeding characterization over a broad spectral range in a single experimental configuration.

In this Letter, we present a self-referencing linear-optical method to completely characterize the temporal-mode state of broadband single photons. This approach, based on spectral shearing interferometry (SSI) [19], enables the characterization of the single-photon spectral-temporal wave function using electro-optic spectral shearing [24] and triggered single-photon spectral measurements [25]. The coincident detection of the spectral measurements with a trigger event is a key difference between our approach and standard SSI techniques, which employ a single spectrally resolved detector. Direct characterization of single-photon pulses after heralding [26] excludes optical and detector noise in the signal mode from the reconstruction and could also be used to characterize conditionally prepared single-photon states from an entangled photon pair [23]. The fact that no additional optical fields besides the test pulse are

utilized implies that this technique is applicable across a broad range of wavelengths. Furthermore, this method does not require scanning of a reference field or spectral measurement to achieve complete state reconstruction, which enables real-time feedback for source optimization.

The state of an ensemble of identically prepared single photons is given by the electromagnetic field mode function that the photons occupy. We presume that the transverse-spatial and polarization state of the photons are known and focus on the pulse mode structure, encapsulated by the complex-valued temporal-mode function  $\psi(t)$  for a pure state. The temporal mode function is interpreted as the temporal wave function, which is a solution to the wave equation in the slowly-varying-envelope approximation [10,27]. In the following, we utilize the spectral representation of the pulse mode, given by the Fourier transform  $\tilde{\psi}(\omega) = \mathcal{F}\{\psi(t)\}$ , since the techniques discussed involve measurements in the spectral domain. Thus, the state of the electromagnetic field when there is a single photon occupying the spectral-temporal mode,  $\tilde{\psi}(\omega)$ , can be expressed by

$$|1\rangle_{\psi} = \int d\omega \tilde{\psi}(\omega) \hat{a}^{\dagger}(\omega) |0\rangle, \quad (1)$$

where  $\hat{a}^{\dagger}(\omega)$  is a field operator creating a single monochromatic photon of frequency  $\omega$  and  $|0\rangle$  is the vacuum state of the field.

The complete characterization of the single-photon state amounts to the measurement of the complex-valued spectral amplitude  $\tilde{\psi}(\omega)$ , which requires the reconstruction of both the magnitude of the spectral amplitude  $|\tilde{\psi}(\omega)|$  and the spectral phase  $\phi(\omega) = \text{Arg}[\tilde{\psi}(\omega)]$ . The spectral amplitude can be determined directly through acquisition of the spectrum

$$S(\omega) = \langle \hat{a}^{\dagger}(\omega) \hat{a}(\omega) \rangle = |\tilde{\psi}(\omega)|^2, \quad (2)$$

where angle brackets imply an ensemble average and the second equality arises from the state in Eq. (1). Single-photon spectral detection can be achieved by frequency-to-time mapping and time-resolved detection as recently demonstrated in both the visible and telecommunications spectral ranges [25,28]. The determination of the spectral phase  $\phi(\omega)$  is more challenging, and at optical frequencies a nonstationary process is necessary [29]. Methods to extract the spectral phase often rely on spectral interferometry [17], where the pulse under test is interfered with either a reference pulse or a modified copy of the pulse itself. This is followed by spectrally resolved detection, allowing the reconstruction of the spectral phase with a Fourier analysis.

The protocol for obtaining the spectral phase using SSI is outlined in Fig. 1 [17]. This involves splitting the pulse at a 50:50 beam splitter, applying a constant spectral translation, or spectral shear  $\Omega$ , to one of the copies and a

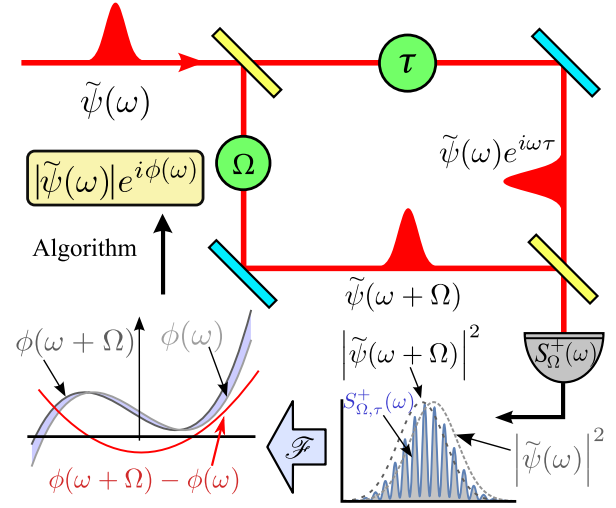


FIG. 1. Measurement principle. Clockwise: The test pulse, in a spectral mode determined by the unknown function  $\tilde{\psi}(\omega)$ , enters a Mach-Zehnder interferometer, in which one arm receives a spectral shear  $\Omega$  and the other a relative time delay  $\tau$ . Spectrally resolved detection reveals an interference pattern  $S_{\Omega, \tau}^{\pm}(\omega)$ . A Fourier analysis of the observed interference pattern enables the extraction of  $\phi(\omega + \Omega) - \phi(\omega)$  (solid red curve) and thus the determination of  $\phi(\omega)$ . The full amplitude and phase of the single-photon-occupied mode can be computationally reconstructed.

temporal delay  $\tau$  to the other, recombining the two at a beam splitter, and measuring the resulting spectral interference pattern. For a single-photon pulse in a mode given by  $\tilde{\psi}(\omega)$ , the intensities at the outputs of the interferometer are

$$S_{\Omega, \tau}^{\pm}(\omega) = \frac{1}{4} \{ S(\omega) + S(\omega + \Omega) \pm 2\text{Re}[\tilde{\psi}(\omega) \tilde{\psi}^*(\omega + \Omega) e^{i\omega\tau}] \}, \quad (3)$$

where  $S(\omega)$  is the spectral intensity of the original pulse. The interferogram  $S_{\Omega, \tau}^{\pm}(\omega)$  (Fig. 2, inset) contains information about the spectral phase difference  $\phi(\omega + \Omega) - \phi(\omega)$ . If  $\Omega$  and  $\tau$  are known, the spectral phase can be extracted from a single interferogram using Fourier-transform-based algorithms [17,30], although multiple acquisitions may be processed together to improve the reliability of the reconstruction.

A method of obtaining the spectral shift  $\Omega$  that is independent of the intensity of the test pulse, and therefore feasible at the single-photon level, is direct linear temporal phase modulation. Recently, this has been demonstrated optomechanically [31] and with cross phase modulation driven by a strong pump field [32]. Frequency translation of a single-photon pulse can also be achieved using electro-optic phase modulation [24], forming the basis of electro-optic spectral-shearing interferometry (EOSI), which has been successfully used to characterize classical light pulses [33]. Here we use the electro-optic approach, with a

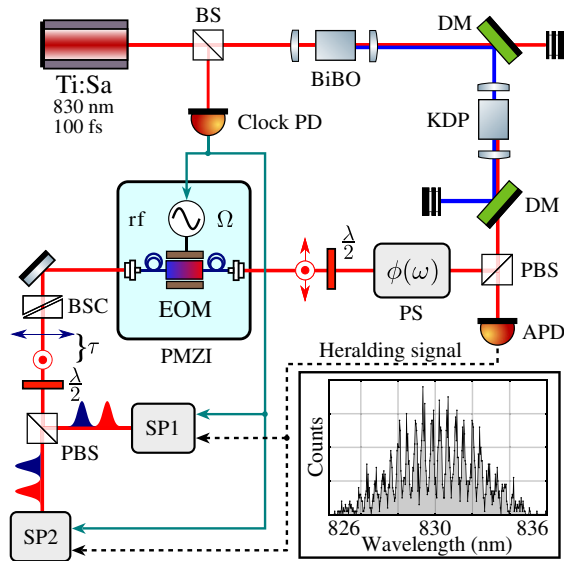


FIG. 2. Experimental setup. The second harmonic of a Ti:sapphire laser (Spectra-Physics Tsunami, 830 nm center wavelength, 80 MHz repetition rate) pumps a spontaneous parametric down-conversion source of broadband heralded single photons. BS, pick-off beam splitter. Clock PD, fast photodiode used to trigger the experiment clock. DM, dichroic mirror. PBS, polarizing beam splitter. APD, avalanche photodiode used to herald a single photon in the signal arm. PS, pulse shaper. PMZI, polarization Mach-Zehnder interferometer.  $\lambda/2$ , half-wave plate. EOM, electro-optic modulator. rf, 10 GHz radio frequency source. BSC, Babinet-Soleil compensator. SP, spectrometer. Electro-optically modulated (unmodulated) polarization is indicated by in-plane (out-of-plane) arrows. Inset: Typical heralded single-photon spectral interferogram at the output of the EOSI acquired in 20 s with approximately 120 Hz coincidence count rate.

lithium-niobate-waveguide electro-optic phase modulator [24]. Electro-optic spectral shearing offers several advantages that make it suitable for SSI. The spectral shear can be realized uniformly over a large wavelength range using a single device and is independent of the incident pulse shape. Hence, only basic knowledge about the input mode, such as wavelength compatibility with the setup, is required, and the same experimental configuration can accurately characterize any of a diverse range of input pulses [34].

The experimental setup for the single-photon mode reconstruction is depicted in Fig. 2. Broadband single photons [830 nm central wavelength with 8 nm full width at half maximum (FWHM) bandwidth], generated by frequency-degenerate spontaneous parametric down-conversion within a potassium dihydrogen phosphate (KDP) crystal pumped at 80 MHz repetition rate, are heralded in a spectrally pure pulse mode [35]. Heralding the photon in a pure state is crucial to the success of the inversion algorithm, which assumes the light under investigation occupies a single temporal mode. This particular source is engineered to generate heralded single photons in a

spectrally pure mode without needing to filter the herald, and hence unheralded light is spectrally coherent, yielding the same reconstruction as the heralded light. The non-classical nature of the reconstructed pulses is encapsulated by the degree of second-order coherence,  $g^{(2)}(0) = 0.06 \pm 0.04$ , measured at the output of the device using the same detectors as in the reconstruction [36]. The low value of  $g^{(2)}(0)$  indicates the single-photon population of the pulses. The broadband signal photon was separated from the idler at a polarizing beam splitter (PBS) and routed, using a single-mode fiber, to a home-built pulse shaper (PS) capable of imprinting an arbitrary spectral phase. As well as compensating for the spectral phase introduced by the EOSI device itself and propagation through various optical elements between the KDP crystal and interferometer, the PS enables the device to be tested with pulses having various phase profiles, where the phase may exhibit pathological behavior [34]. The heralding idler photon was detected by a single-mode-fiber-coupled single-photon-counting module. After the PS, the polarization was rotated to  $45^\circ$  and injected into a polarization Mach-Zehnder interferometer (PMZI), in which the two interferometer arms comprise the two polarization modes of the birefringent setup. The PMZI consists of a polarization-maintaining fiber-coupled electro-optic phase modulator (EOM) driven by a 10 GHz sinusoidal radio-frequency (rf) signal synchronized with the pump laser pulse train, where one of the polarization components was spectrally sheared by  $\Delta\lambda = 0.58 \pm 0.02$  nm. Subsequently, a calcite Babinet-Soleil compensator was used to adjust the time delay  $\tau$  between the two orthogonal polarizations. The value of  $\tau$  is independently determined by an interferometric method with classical light [34]. The accurate calibration of  $\tau$  is necessary for a reliable spectral phase reconstruction. The PMZI is closed using a half-wave plate and a PBS, with PBS outputs coupled by single-mode optical fibers to two time-resolved single-photon-counting spectrometers for the acquisition of the heralded single-photon spectrograms [25]. This common-path arrangement provides the long-term-stable interference needed to acquire sufficient photon counts to build up the interferogram.

We characterize the path leading up to the PMZI by reconstructing the spectral phase of the heralded signal photon that passes through several dispersive elements, including several meters of optical fiber, before entering the PMZI (not shown in Fig. 2) and then compensate for the quadratic dispersion using the PS. Figure 3(a) shows the spectral amplitude (1) and phases of the uncompensated (2) and compensated (3) single-photon pulses. A large positive quadratic spectral phase of  $(8.7 \pm 0.1) \times 10^4$  fs<sup>2</sup> and a small cubic component of  $(5.0 \pm 1.0) \times 10^5$  fs<sup>3</sup> are found. Applying this quadratic spectral phase with the opposite sign using the PS and reconstructing the spectral phase shows a compensation of the quadratic phase, while the cubic component still remains. The extracted quadratic phase

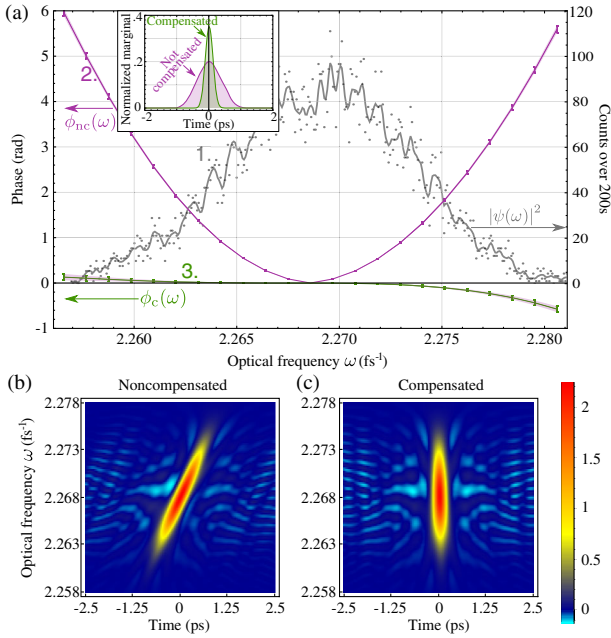


FIG. 3. Top: Reconstructed phases for unshaped ( $\phi_{nc}$ , 2) and compensated for quadratic phase ( $\phi_c$ , 3) cases. The grayscale plot (1) assigned to the right-hand scale represents the single-photon spectral intensity. The gray scatter plot shows raw counts per frequency mode, with a low-pass filter giving the solid gray line. Inset: Absolute value of the temporal wave function. Bottom: Chronocyclic Wigner functions of (b) an unshaped pulse and (c) compensated for excess quadratic phase.

coefficient in the corrected case is  $(-1.3 \pm 0.9) \times 10^3 \text{ fs}^2$ , indicating close agreement between the phase applied on the pulse shaper and that measured by the reconstruction.

Using the measured spectrum shown in Fig. 3(a) and the reconstructed phases, it is possible to calculate the single-photon temporal wave function  $\psi(t)$  with the magnitude shown inset. When compensating the quadratic dispersion, we obtain a flat spectral phase corresponding to a temporal pulse compressed to its transform-limited duration. The amount of remaining cubic phase is small enough to not significantly change the temporal waveform. This can be seen in Figs. 3(b) and 3(c), which show the chronocyclic Wigner distributions for these two pulses. This representation constitutes a quasiprobability distribution in the time-frequency space of the pulse and allows spectral-temporal correlations, such as those brought about by the spectral phase, to be visualized [37]. The delay in arrival time of the higher-frequency components of the pulse, brought about by the second-order spectral phase, can be seen clearly in the tilted Wigner function [Fig. 3(b)], while the transform-limited pulse duration is manifest in Fig. 3(c).

To further demonstrate the versatility of the single-photon EOSI, the PS was used to manipulate single photons into one of two states with spectral phase profiles shown in Fig. 4(a) 1 and 2, termed “V” and “ $\Lambda$  phases,”

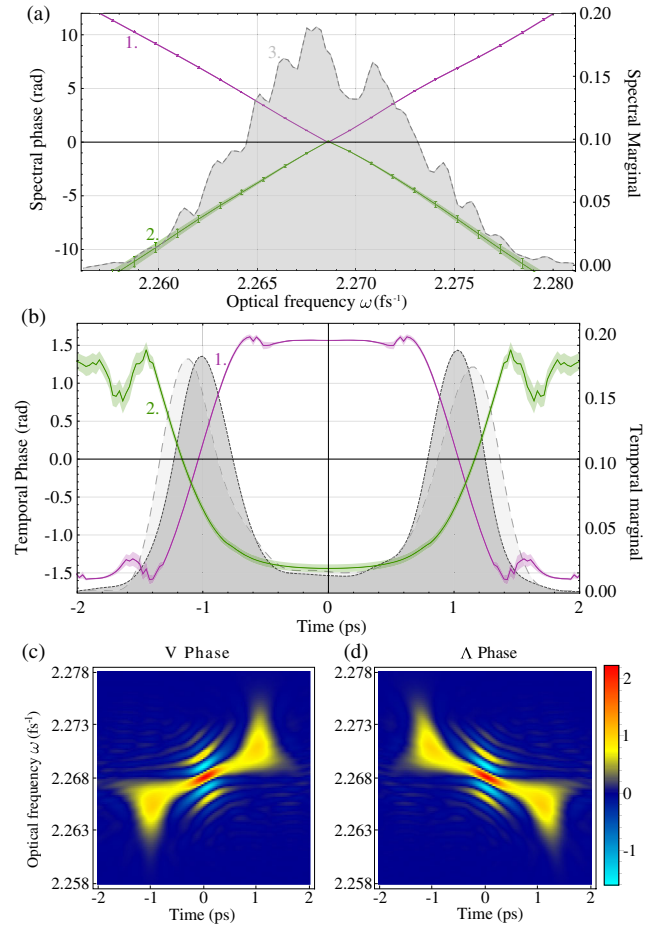


FIG. 4. (a) Reconstructed spectral phase profiles of pulses with an applied V phase (1, purple) and  $\Lambda$  phase (2, green), with the single-photon spectrum shown in grayscale (3). (b) Reconstructed temporal phases for the V phase (1, purple) and  $\Lambda$  phase (2, green), as well as the temporal profile, showing binodal temporal distribution. (c) Chronocyclic Wigner functions of the V-phase pulse and (d)  $\Lambda$ -phase pulse.

respectively. Note that the linear spectral phase  $\phi(\omega) = \omega T$  can be viewed as a time delay  $T$ . The pulses produced by the V and  $\Lambda$  spectral phases have binodal temporal intensity profiles, caused by relative delays between the high- and low-frequency spectral components (with opposite sign for the two different phase profiles). The V ( $\Lambda$ ) phase results in the low- (high-) frequency components arriving before the high- (low-) frequency components of the pulse. This delay is introduced by applying linear spectral phases of opposite sign on each half of the pulse spectrum using the PS [38]. The V- and  $\Lambda$ -phase pulses thus have the property that they have identical spectral and temporal intensities but are nearly orthogonal despite being created from the same initial resource through phase-only operations. Distinguishing these two states can therefore be achieved only with phase-sensitive measurements.

Figure 4(a) shows the reconstructed phase profiles of the two pulses, providing excellent agreement with the phase

written onto the pulse shaper. The reconstructed linear phase coefficients are found to be  $T = 1050 \pm 100$  fs and  $T = -1100 \pm 200$  fs for the  $V$  and  $\Lambda$  phases, respectively. Using the experimentally measured single-photon spectrum, the reconstructed binodal temporal intensity distributions and temporal phases are shown in Fig. 4(b), as well as the chronocyclic Wigner functions of the two pulses, Figs. 4(c) and 4(d). The Wigner functions show the delays between high- and low-frequency components of the pulses and the coherences between them. Although the spectral and temporal intensity distributions are indistinguishable, the modes are indeed nearly orthogonal, with an overlap of  $0.06 \pm 0.01$ .

In summary, we have demonstrated a self-referencing technique to reconstruct the spectral-temporal state of a pulsed, heralded single-photon source. This method is applicable across a wide range of wavelengths and pulse characteristics, and no optical reference fields are required. The only *a priori* knowledge needed is that associated with the technical compatibility of the pulses with the optics and detectors. The full characterization of an arbitrary pure state can be performed in a single experimental configuration without modifying the apparatus. The spectral shear  $\Omega$  can easily be reconfigured, enabling a more robust reconstruction of complicated or even partially mixed pulse trains [34,39]. Because our approach to pulse characterization is based upon the measurement of the first-order correlation function [34], it is not limited to the measurement of single-photon pulses and can be employed to characterize other triggered low-intensity pulsed sources, e.g., a weak coherent state from a pulsed laser. Furthermore, multiple single-photon EOSI devices could be used to characterize multiphoton states displaying high-dimensional spectral-temporal entanglement. Our device has wide applications in single-photon source and detector characterization and quantum metrology. The characterization of single-photon sources of typical luminosity is rapid enough to enable real-time feedback in source optimization. We anticipate that future experiments will also utilize this technology for more diverse purposes such as spectral-temporal entanglement characterization and state purity determination.

We are grateful to C. Dorrer, C. Radzewicz, M. G. Raymer, and I. A. Walmsley for fruitful discussions. This project has received funding from the European Union's Horizon 2020 research and innovation program under Grant Agreement No. 665148, the United Kingdom Defense Science and Technology Laboratory (DSTL) under Contract No. DSTLX-100092545, and the National Science Foundation under Grant No. 1620822. This work was partially funded by the HOMING program of the Foundation for Polish Science (Project No. Homing/2016-1/4) cofinanced by the European Union under the European Regional Development Fund.

A. D. and V. T. contributed equally to this work.

- [1] A. I. Lvovsky and M. G. Raymer, *Rev. Mod. Phys.* **81**, 299 (2009).
- [2] J. L. O'Brien, A. Furusawa, and J. Vučković, *Nat. Photonics* **3**, 687 (2009).
- [3] I. Białynicki-Birula, *Acta Phys. Pol. A* **86**, 97 (1994).
- [4] J. Sipe, *Phys. Rev. A* **52**, 1875 (1995).
- [5] B. J. Smith and M. G. Raymer, *New J. Phys.* **9**, 414 (2007).
- [6] H. Sasada and M. Okamoto, *Phys. Rev. A* **68**, 012323 (2003).
- [7] V. Thiel, J. Roslund, P. Jian, C. Fabre, and N. Treps, *Quantum Sci. Technol.* **2**, 034008 (2017).
- [8] T. B. Pittman, B. C. Jacobs, and J. D. Franson, *Phys. Rev. Lett.* **88**, 257902 (2002).
- [9] J. Nunn, L. J. Wright, C. Söller, L. Zhang, I. A. Walmsley, and B. J. Smith, *Opt. Express* **21**, 15959 (2013).
- [10] B. Brecht, D. V. Reddy, C. Silberhorn, and M. G. Raymer, *Phys. Rev. X* **5**, 041017 (2015).
- [11] M. Hentschel, R. Kienberger, C. Spielmann, G. A. Reider, N. Milosevic, T. Brabec, P. Corkum, U. Heinzmann, M. Drescher, and F. Krausz, *Nature (London)* **414**, 509 (2001).
- [12] S. T. Cundiff and S. Mukamel, *Phys. Today* **66**, No. 7, 44 (2013).
- [13] A. M. Weiner, *Opt. Commun.* **284**, 3669 (2011).
- [14] J. Roslund, R. M. de Araujo, S. Jiang, C. Fabre, and N. Treps, *Nat. Photonics* **8**, 109 (2014).
- [15] V. Giovannetti, S. Lloyd, and L. Maccone, *Nat. Photonics* **5**, 222 (2011).
- [16] A. R. Dixon, Z. Yuan, J. Dynes, A. Sharpe, and A. Shields, *Appl. Phys. Lett.* **96**, 161102 (2010).
- [17] I. A. Walmsley and C. Dorrer, *Adv. Opt. Photonics* **1**, 308 (2009).
- [18] D. J. Kane and R. Trebino, *Opt. Lett.* **18**, 823 (1993).
- [19] C. Iaconis and I. A. Walmsley, *Opt. Lett.* **23**, 792 (1998).
- [20] W. Wasilewski, P. Kolenderski, and R. Frankowski, *Phys. Rev. Lett.* **99**, 123601 (2007).
- [21] C. Polycarpou, K. N. Cassemiro, G. Venturi, A. Zavatta, and M. Bellini, *Phys. Rev. Lett.* **109**, 053602 (2012).
- [22] Z. Qin, A. S. Prasad, T. Brannan, A. MacRae, A. Lezama, and A. I. Lvovsky, *Light Sci. Appl.* **4**, e298 (2015).
- [23] V. Ansari, J. M. Donohue, M. Allgaier, L. Sansoni, B. Brecht, J. Roslund, N. Treps, G. Harder, and C. Silberhorn, *Phys. Rev. Lett.* **120**, 213601 (2018).
- [24] L. J. Wright, M. Karpiński, C. Söller, and B. J. Smith, *Phys. Rev. Lett.* **118**, 023601 (2017).
- [25] A. Davis, P. Saulnier, M. Karpiński, and B. J. Smith, *Opt. Express* **25**, 12804 (2017).
- [26] V. Ansari *et al.*, *Opt. Express* **26**, 2764 (2018).
- [27] J.-C. Diels and W. Rudolph, *Ultrashort Laser Pulse Phenomena* (Academic, New York, 2006).
- [28] M. Avenhaus, A. Eckstein, P. J. Mosley, and C. Silberhorn, *Opt. Lett.* **34**, 2873 (2009).
- [29] V. Wong and I. A. Walmsley, *Opt. Lett.* **19**, 287 (1994).
- [30] C. Dorrer and I. A. Walmsley, *J. Opt. Soc. Am. B* **19**, 1019 (2002).
- [31] L. Fan, C.-L. Zou, M. Poot, R. Cheng, X. Guo, X. Han, and H. X. Tang, *Nat. Photonics* **10**, 766 (2016).
- [32] N. Matsuda, *Sci. Adv.* **2**, e1501223 (2016).
- [33] C. Dorrer and I. Kang, *Opt. Lett.* **28**, 477 (2003).
- [34] A. Davis, V. Thiel, M. Karpiński, and B. J. Smith, *Phys. Rev. A* **98**, 023840 (2018).

- [35] P. J. Mosley, J. S. Lundeen, B. J. Smith, P. Wasylczyk, A. B. U'Ren, C. Silberhorn, and I. A. Walmsley, *Phys. Rev. Lett.* **100**, 133601 (2008).
- [36] R. Loudon, *The Quantum Theory of Light* (Oxford University, New York, 2000).
- [37] J. Paye, *IEEE J. Quantum Electron.* **28**, 2262 (1992).
- [38] The phases were applied on top of the quadratic phase correction that compresses the temporal wave function to the transform limit.
- [39] M. Mang, C. Bourassim-Bouchet, I. Gianani, and I. Walmsley, *Opt. Lett.* **38**, 6142 (2013).